

1 **Title:**

2 Genome-wide markers untangle the green-lizard radiation in the Aegean Sea and
3 support a rare biogeographical pattern

4

5 **Short running title:** *Lacerta* phylogeography in the Aegean

6

7 **Article type:** Research paper

8

9 **Authors' names:**

10 Panagiotis Kornilios^{1,2,3†}; Evanthia Thanou^{1,3}; Petros Lymberakis⁴; Çetin Ilgaz^{5,6}; Yusuf
11 Kumlutaş^{5,6}; Adam Leaché^{1,7}

12

13 **Authors' research addresses:**

14 1 Department of Biology, University of Washington, Box 351800, Seattle, WA 98195-
15 1800, USA

16 2 Institute of Evolutionary Biology (CSIC - Universitat Pompeu Fabra), Passeig
17 Marítim de la Barceloneta 37-49, E-08003 Barcelona, Spain

18 3 The Molecular Ecology Backshop, G. Lekka 16, GR-26300, Loutraki, Greece

19 4 Natural History Museum of Crete, University of Crete, Knossou Ave., GR-71409
20 Irakleio, Crete, Greece

21 5 Department of Biology, Faculty of Science, Dokuz Eylül University, 35160 Buca-
22 İzmir, Turkey

23 6 Research and Application Center for Fauna Flora, Dokuz Eylul University, 35160
24 Buca-İzmir, Turkey.

25 7 Burke Museum of Natural History and Culture, University of Washington, Box
26 353010, Seattle, WA 98195-3010, USA

27

28 † **Corresponding author:** Department of Biology, University of Washington, Box
29 351800, Seattle, WA 98195-1800, USA, email: korniliospanagiotis@gmail.com,
30 korniliospan@yahoo.gr

31

32 **Word count:** Abstract – 276

33 Main Text + references = 7741

34 Estimated number of pages required by figures and tables: 4

36 **Abstract**

37

38 **Aim:** The Aegean Sea constitutes a major biogeographic barrier between the European
39 and Asian continents and several models of diversification in the Aegean have been
40 documented. Here we test three of those models for the Aegean green-lizards (*Lacerta*
41 *trilineata–pamphylica* group): Vicariance vs. Overland Dispersal vs. Island Stepping-
42 stone Dispersal. We investigate these hypotheses and complement our knowledge on
43 the impact of the Aegean Barrier on east Mediterranean taxa.

44

45 **Location:** Aegean Sea, east Mediterranean

46

47 **Taxon:** *Lacerta* lizards

48

49 **Methods:** We analysed ddRAD loci (double-digest restriction-site-associated DNA) to
50 estimate species-trees under coalescent models and maximum likelihood trees using
51 concatenation. We performed hierarchical population structure analyses and inferred
52 ancestral distribution-areas. We also sequenced the complete cytochrome *b* gene and
53 produced a time-calibrated mtDNA gene-tree tree to conduct a critical comparison with
54 previous studies.

55

56 **Results:** Aegean green-lizards diverged into four main groups in parallel during the
57 Late Pliocene with distributions to the East and West of the Aegean. The Eastern group
58 includes *Lacerta pamphylica* and East Aegean *L. trilineata*, while the Western group
59 contains the Central Cyclades populations and the remaining populations of the Balkan
60 Peninsula. The Aegean green-lizards' ancestor occurred in Anatolia, while the West
61 lineage ancestor occurred in the Central Cyclades islands, revealing a dispersal between
62 the two regions. The radiations of all major green-lizard groups, including
63 *trilineata+pamphylica*, occurred in parallel in the Late Pliocene.

64

65 **Main Conclusions:** In contrast to previously suggested biogeographical hypotheses for
66 the group, based on mtDNA, the Island Stepping-stone Dispersal scenario is strongly
67 supported. Green lizards offer a rare paradigm of diversification in the Aegean, where
68 populations largely expanded their geographical distribution and crossed the Aegean
69 Barrier by using the central Aegean islands as stepping stones.

70

71 **KEYWORDS:** Aegean Sea barrier, Anatolia, ddRAD, East Mediterranean, Genome
72 wide SNPs, Lacertidae, Mid-Aegean Trench, Overseas dispersal, phylogeography,
73 SNAPP coalescence
74

76 1. INTRODUCTION

77

78 1.1. The Aegean Sea: a biogeographic barrier and a bridge

79

80 The Aegean Sea constitutes a major contemporary barrier to biotic exchange between
81 the continents of Asia and Europe. However, this has not always been the case. During
82 the early and middle Miocene, this region was in fact a united landmass called the Agäis
83 or Aegaeis (Creutzburg, 1963). This land included what we recognise today as the
84 southern Balkan Peninsula in the west, Anatolia in the east and the Aegean itself, which
85 at that time formed an unbroken plain (Figure 1). This configuration permitted cross-
86 continental dispersal and uninterrupted geographic distributions of flora and fauna
87 throughout the area.

88 The fragmentation of this landmass and the formation of one of the most
89 important biogeographical barriers in the region derived from the northward movement
90 and subduction of the African plate beneath the Eurasian plate (Le Pinchon & Angelier,
91 1981). One important consequence of this collision was the intrusion of the sea, which
92 began approximately 12 Ma east of today's Crete (Creutzburg, 1963), moved northward
93 and was complete some 8-9 Ma (Dermitzakis, 1990) (Figure 1). This sea barrier, often
94 termed the Mid-Aegean Trench (MAT; Poulakakis et al., 2003), represented the first
95 form of the Aegean Sea. Trenches are long, narrow depressions on the seafloor that
96 form at the meeting points of tectonic plates. For example, the Hellenic Trench was
97 formed in the south of the Aegean region from the collision of the African and Eurasian
98 plates (Le Pinchon & Angelier, 1981). Since the Mid-Aegean Trench is not technically
99 a trench, we refer to it as the Aegean Barrier (AB).

100 Palaeogeographic reconstructions some 8 Ma show that the eastern and western
101 parts of the Aegean were separated by the AB, while the present central Aegean islands
102 formed a united landmass connected to the west mainland, i.e. the present Balkan
103 Peninsula. Crete was also isolated but in the form of a chain of smaller islands
104 (Dermitzakis & Papanikolanou, 1981; Figure 1). During the late Pliocene, the
105 palaeogeographic reconstructions converge to great extent but with some
106 differentiations. Dermitzakis and Papanikolanou (1981) present a map of the Aegean at
107 approximately 3.5 Ma, which shows no connections between the east and the west (the
108 AB remained undisrupted), and the central Aegean islands were still forming a
109 landmass connected to the mainland. Creutzburg (1963) presents a map of the late
110 Pliocene, with no precise dates in Ma, according to which there was a narrow
111 landbridge that connected present Anatolia and the central Aegean landmass (the AB
112 was disrupted), while the latter was separated from the mainland by a narrow sea strait.

113 In both studies, Crete remained isolated, while the Peloponnese was disconnected from
114 the rest of the Balkan Peninsula (Figure 1). Finally, Anastasakis, Piper, Dermitzakis and
115 Karakitsios (2006) show that during the early Pliocene, the central Aegean landmass
116 was connected to the mainland, but it was disconnected during the late Pliocene, again
117 with no precise dates in Ma. The consensus of all these depictions is that until the late
118 Pliocene the east and west Aegean most probably remained isolated by the AB and if
119 there were actual landbridges between them, they must have been very limited in space
120 and time. Additionally, the central Aegean islands formed a large landmass connected to
121 the present Balkan Peninsula until the transition from the late to early Pliocene, when
122 they were disconnected. During the Pleistocene, the geological configurations of the
123 Aegean were similar to the present ones. However, the oscillating climatic conditions
124 during the glacial and interglacial periods led to sea-level fluctuations, which connected
125 and disconnected islands with their neighbouring mainlands. Accordingly, the central
126 Aegean islands at times formed larger islands or were even united in one landmass,
127 which never re-connected with the Balkan mainland because of the great sea depth in
128 this area (Anastasakis et al., 2006).

129 In a biogeographical context, animal taxa have either historically not overcome
130 the AB and are confined to one of the two sides, or can be found on both sides. In the
131 latter cases, five models of diversification can be observed:

132

- 133 1. Vicariance: an old distribution becomes fragmented because of the AB
134 formation.
- 135 2. Overland Dispersal: Dispersal from one side to the other following a route in the
136 north around the AB.
- 137 3. Single Crossings: Taxa have the bulk of their distribution on one side but appear
138 on a single or few locations on the other.
- 139 4. Human-mediated introductions to one or multiple locations.
- 140 5. Island Stepping-stone Dispersal from one side of the AB to the other and
141 subsequent expansion. This rare pattern has been inferred for very few invertebrates in
142 recent studies (Allegrucci, Trucchi & Sbordoni, 2011; Kornilios, Thanou, Kapli,
143 Parmakelis & Chatzaki, 2016), but so far it has not been observed in terrestrial
144 vertebrates.

145

146 **1.2. Study system and biogeographical hypotheses**

147

148 Reptiles and especially lizards have long been used as models for the study of
149 speciation processes and phylogeographical patterns, with the family Lacertidae being

150 the most commonly studied group (Camargo, Sinervo & Sites, 2010). The west
151 Eurasian genus *Lacerta* includes eight recognized species forming three species-groups.
152 The east Mediterranean *L. trilineata* group comprises *L. media* Lantz & Cyrén, 1920,
153 which is morphologically and genetically distinct (Ahmadzadeh et al., 2013), *L.*
154 *pamphylica* Schmidtler, 1975 and *L. trilineata* Bedriaga, 1886.

155 The *trilineata+pamphylica* clade is an ideal model to test biogeographical
156 hypotheses regarding the Aegean region. It presents significant morphological and
157 genetic variation, has a large distribution on both sides of the AB and is found on all
158 major island-groups (Figure 1). Mitochondrial phylogenies converge to an eastern
159 (Anatolian) origin of the group, but with contradicting conclusions regarding the timing
160 and mode of divergence (Ahmadzadeh et al., 2013; Sagonas et al., 2014). There is no
161 prior knowledge on whether Aegean green-lizards are good or bad dispersers, but
162 limited studies on other *Lacerta* species point to low dispersal capacities and a male-
163 biased dispersal mode (Böhme, Schneeweiss, Fritz, Schlegel & Berendonk, 2006).

164 Here we test three alternative hypotheses regarding the historical biogeography of
165 this group to draw broader conclusions on the patterns observed in the Aegean region,
166 focusing on the role of the AB: Vicariance (V) vs. Overland Dispersal (OD) vs. Island
167 Stepping-stone Dispersal (ISD) (see Appendix S1 in Supporting Information for a
168 schematic presentation of the three models). Since the group presents an old radiation
169 and is largely distributed on both sides of the AB (Ahmadzadeh et al., 2013; Sagonas et
170 al., 2014), the human mediated and single-crossing scenaria are excluded. We test
171 biogeographic models, by investigating the population structure, phylogeny, and
172 biogeography of the species group using independent loci from across the genome, with
173 a double-digest restriction-site-associated DNA sequencing approach (ddRADseq;
174 Peterson, Weber, Kay, Fisher & Hoekstra, 2012). We compare our results with an
175 expanded mtDNA gene tree for straightforward comparisons with published studies.

176

177 2. MATERIALS AND METHODS

178

179 2.1. Sampling

180

181 Sampling was designed to represent genetic diversity from *L. trilineata* and *L.*
182 *pamphylica*, all involved biogeographical regions and all known mitochondrial lineages
183 (Figure 1b). Specimen data (working codes, sampling localities and GenBank
184 Accession Numbers) are given in Table 1, while sampling localities are also shown in
185 Figure 1.

186

187 2.2. Genomic data: ddRAD library preparation, sequencing and bioinformatics

188

189 We collected ddRADseq data following the protocol, barcode-adaptors and indices of
190 Peterson et al. (2012). Briefly, we double-digested genomic DNA with enzymes SbfI
191 and MspI. Fragments were ligated with barcoded Illumina adapters, samples were
192 pooled and, after each pool of eight samples was size-selected for fragments in the
193 range of 415 - 515 bp, they were ligated with Illumina multiplexing indices. Sequencing
194 was done on a single Illumina HiSeq 4000 lane (50 bp single-end read).

195

196 We processed raw Illumina reads using the program iPyRAD v.0.7.8 (Eaton,
197 2014). We demultiplexed samples using their unique barcode and index, and reduced
198 each read to 39 bp after removal of the 6 bp restriction site overhang and the 5 bp
199 barcode. Within the iPyRAD pipeline, the filtered reads for each sample were clustered
200 using VSEARCH v.2.4.3 (Rognes, Flouri, Nichols, Quince & Mahé, 2016) and aligned
201 with MUSCLE v.3.8.31 (Edgar, 2004).

202

203 We generated final datasets using three thresholds for the minimum number of
204 individuals with data for a given locus: D0 (0% missing data, i.e. all loci present for all
205 samples), D10 (10% missing data, all loci present for at least 90% of the samples) and
206 D25 (25% missing data). Two types of final data-matrices were generated for different
207 downstream analyses that included either the entire ddRAD locus (variable and
208 invariant sites combined: “ddRAD” datasets) or by choosing one random SNP from
209 each putatively unlinked locus (“uSNP” datasets). Each time a new dataset was
210 generated the iPyRAD pipeline ran again for the specific set. Details regarding the
211 parameters used for de-multiplexing and a summary of all resulting datasets from the
212 iPyRAD pipeline are provided in Appendix S2, while a summary of this information is
213 given in Table 2.

212

213 2.3. Genomic data: genetic clusters and admixture

214

215 Genetic structure within *trilineata+pamphylica* was inferred with two approaches using
216 the uSNP-D0 datafile: Discriminant Analysis of Principal Components (DAPC;
217 Jombart, Devillard & Balloux, 2010) using the R package ADEGENET (Jombart, 2008)
218 and the Bayesian clustering analysis implemented in STRUCTURE v.2.3.4 (Pritchard,
219 Stephens, & Donnelly, 2000). The optimal number of clusters (from 1 to 12) was
220 estimated with the find.cluster function in ADEGENET, and the Bayesian Information
221 Criterion (BIC) was used to select the optimal number of groups. To avoid overfitting,
222 we used the a-score function to determine the appropriate number of principal
223 components.

224 We used STRUCTURE to infer the number of genetic clusters K (1 to 12) and
225 potential admixture. Analyses were performed with five runs of 500,000 iterations each
226 (250,000 burn-in), with correlated allele frequencies and under the admixture model
227 (Falush, Stephens, & Pritchard, 2003). We processed runs with the ‘greedy’ option and
228 2,000 random input orders in the CLUMPAK online web server (Kopelm, Mayzel,
229 Jakobsson, Rosenberg & Mayrose, 2015) and evaluated the optimal K following
230 Evanno, Regnaut & Goudet (2005). We used a hierarchical approach to determine
231 whether additional structure was present in inferred groups by repeating STRUCTURE
232 analyses using subsets of the data (see details in Results). We repeated this procedure
233 until no additional population structure was supported ($K = 1$).

234

235 **2.4. Genomic data: coalescence species trees and concatenated ddRAD loci**

236

237 We estimated a species tree under the Bayesian multispecies coalescent framework of
238 SNAPP v1.3 (SNP and AFLP Package for Phylogenetic analysis; Bryant, Bouckaert,
239 Felsenstein, Rosenberg & RoyChoudhury, 2012) implemented in BEAST2 v2.4
240 (Bayesian Evolutionary Analysis Sampling Trees; Bouckaert et al., 2014). To avoid
241 model violations (SNAPP assumes no gene flow), we excluded admixed individuals
242 (membership probability <99% according to STRUCTURE). The final dataset included
243 unlinked biallelic SNPs (biallelic uSNP-D10), no outgroup and the genetic-clustering
244 results used for population assignments. Since SNAPP is computationally intensive,
245 each population included 2-5 individuals, to a total of 22. Mutation rates (u , v) were
246 both fixed at 1.

247

248 SNAPP uses a Yule prior with parameter lambda (λ) representing the speciation
249 rate. For the λ prior we used a broad gamma distribution with a mean value of 1,000, set
249 as $\alpha \times \beta$ ($\alpha=2$, $\beta=500$). Since λ determines the prior expected height of the tree, we used
250 our non-reduced ddRAD dataset, containing all variable and constant characters, to

251 estimate the tree height (maximum observed divergence between any pair of taxa
252 divided by two). We then utilised Jamie Oaks' script `pyule`
253 (<https://github.com/joaks1/pyule>) to determine the mean value of λ .

254 The theta (θ) prior was also set as a gamma distribution with a mean value of
255 0.001, defined as α/β ($\alpha=25$, $\beta=25,000$). Using this ratio, and since α/β^2 represents the
256 variance, we ensured that the Standard Deviation (SD) was 0.0002. A prior mean θ
257 =0.001 implies 0.1% variation between two randomly sampled alleles in a population.
258 The values used (mean and SD) were estimated from the non-reduced dataset
259 (percentage of polymorphic sites within each of the defined populations).

260 We performed two independent runs with a chain length of 6×10^6 generations,
261 sampling every 1,000 generations. We checked convergence ($ESS > 200$) and determined
262 burnin (10%) with TRACER v1.6 (Rambaut & Drummond, 2007). A maximum clade
263 credibility tree (MCC) was summarized with TreeAnnotator.

264 Phylogenomic relationships among individuals and populations were also inferred
265 using the coalescent method SVDquartets v.1.0 (Chifman & Kubatko, 2014)
266 implemented in PAUP* v.4.0b10 (Phylogenetic Analysis Using Parsimony; Swofford,
267 2003). We evaluated all possible quartets, with and without prior assignment to
268 populations and used non-parametric bootstrapping with 1,000 replicates for the
269 statistical support. Final analyses ran without admixed individuals, *L. viridis* as
270 outgroup and the uSNP-D25 dataset.

271 A maximum likelihood (ML) tree was also constructed using the concatenated
272 ddRAD loci with IQ-TREE1.4.3 (Nguyen, Schmidt, von Haeseler & Minh, 2015). We
273 used the "Auto" option for best-fit substitution model and tested nodal support via SH-
274 aLRT tests (Shimodaira–Hasegawa approximate Likelihood Ratio Test; 1,000
275 replicates) (Guindon et al., 2010) and 1,000 ultrafast bootstrap alignments (Minh,
276 Nguyen & von Haeseler, 2013). We tested several datasets and final analyses ran
277 without admixed individuals, with an outgroup and the ddRAD-D25 dataset.

278

279 **2.5. Genomic data: biogeographical analysis**

280

281 To infer ancestral distribution areas, we employed the Bayesian binary Markov
282 chain Monte Carlo (BBM) implemented in RASP v.3.2 (Reconstruct Ancestral State in
283 Phylogenies; Yu, Harris, Blair & He, 2015). This analysis does not require an
284 ultrametric tree nor considers the branch lengths, while it accepts trees with polytomies.
285 In this context, we used as input the tree from the SVDquartets analysis of individuals,
286 after pruning the outgroup. We assigned the terminal nodes to seven geographical areas
287 that were defined based on the distribution of lineages, the geography and

288 palaeogeography of the region (Figure 1b). We run two independent analyses with ten
289 MCMC chains for 10^7 generations under the JC+G model, states sampled every 100
290 generations, 25% burnin and ancestral ranges allowed to include up to four areas.

291

292 **2.6. Mitochondrial DNA: gene tree analysis and estimation of divergence times**

293

294 The complete mitochondrial cytochrome *b* gene (*cytb*) was PCR-amplified with primers
295 L14910 and H16064 (Burbrink, Lawson & Slowinski, 2000), following standard
296 procedures (e.g. Kyriazi et al., 2013). New sequences were combined with published
297 ones to construct a dataset that included 41 ingroup sequences with a length of 1,137 bp.

298 The mtDNA phylogeny was assessed with ML carried out in IQ-TREE. The
299 analysis ran with the “partitionfinder” and “Auto” options that determine the best
300 partitioning scheme and the best-fit substitution model for each partition (Chernomor,
301 von Haeseler & Minh, 2016). Nodal support was tested via 10,000 SH-aLRT tests,
302 10,000 ultrafast bootstrap alignments and 100 standard bootstrap alignments. We
303 included *L. media* and rooted the tree with *L. agilis*.

304 To infer divergence times and in order to investigate the discrepancies between
305 published studies, we combined our *cytb* sequences with sequences from GenBank to
306 generate the datasets of Ahmadzadeh et al. (2013) and Sagonas et al. (2014).
307 Specifically, we included the same six *Gallotia* and four *Timon* species, but added
308 *Timon lepidus* since the split between this and its sister-species *T. nevadiensis* is the
309 appropriate node to calibrate. Regarding the *Lacerta* representatives, we downloaded all
310 available complete or near-complete *cytb* sequences from all eight species and removed
311 redundant haplotypes. We generated a 1,137 bp dataset of 346 haplotypes and built a
312 ML tree in IQ-TREE. This was, in turn, used to delimit mtDNA clusters with mPTP
313 (Multi-rate Poisson tree processes; Kapli et al., 2017) and generate a final dataset of 45
314 sequences by including one representative from each mtDNA cluster, in order to
315 conform to the Yule model of cladogenesis. We also performed a critical re-analysis of
316 the Sagonas et al. (2014) dataset (Appendix S3).

317 To time-calibrate the phylogeny, we used the same four calibration points and
318 prior probability distributions as in both published studies (details in Appendix S3).
319 Analyses were performed in BEAST v1.8.4 (Drummond, Suchard, Xie & Rambaut,
320 2012), under the uncorrelated lognormal relaxed-clock approach with a Yule tree prior,
321 four runs of 5×10^7 generations and sampling every 1,000 steps. Analyses were carried
322 out in CIPRES science gateway (Miller, Pfeiffer & Schwartz, 2010).

323

324 3. RESULTS

325

326 The ddRAD assemblies included a total of 34 samples, including two *L. viridis*
327 individuals used as outgroups (Table 1). The mtDNA ML phylogeny was built on 47
328 complete *cytb* sequences (41 ingroup), while 31 additional sequences were used in the
329 final molecular clock analysis (Table 1). Details on the ddRAD datasets that were used
330 in the final analyses are shown in Table 2 and Appendix S2.

331

332 3.1. Genetic clusters and admixture

333

334 DAPC returned $K=8$ as the optimal number of clusters (Figure 2b), with a mean
335 assignment probability of 0.97. Cluster analysis with STRUCTURE (Figure 2c)
336 supported $K=2$, but the hierarchical procedure detected additional population genetic
337 structure resulting in a total of nine groups. The two clusters grouped East and West
338 Aegean populations, respectively. The East group was further divided into three groups:
339 *L. pamphylica*, Lesvos island and all remaining East *L. trilineata* populations.
340 Admixture between the last two was found for one of the Turkish specimens located
341 across the island of Lesvos ($Q=0.67$). Analysis of the West group also returned three
342 groups: the Central Cyclades islands, all specimens from Peloponnesos and Crete, and
343 all remaining mainland and island populations. Further genetic clustering was supported
344 within each of the last two groups. In the first case, populations from Peloponnesos and
345 Crete were assigned into two respective clusters, and in the second, three more clusters
346 were identified, the West Cyclades islands, East mainland Greece and adjacent islands,
347 and West mainland Greece and islands. Two individuals from West mainland Greece
348 showed admixture between the last two clusters ($Q=0.85$ and $Q=0.67$).

349

350 3.2. Phylogenomic trees and ancestral distributions

351

352 The MCC tree from SNAPP (Figure 2a) could not resolve the phylogenetic position of
353 the Cretan populations relative to the Peloponnesian ones and the position of the West
354 Cyclades populations relative to the mainland Greece ones. The SVDquartets species-
355 tree favoured the relationship between Crete and east Peloponnesos (Figure 2a). The
356 SVDquartets tree with individuals as terminal branches was very similar to the
357 concatenated ML tree (Figure 3). In all ddRAD-based trees (Figures 2 and 3), two major
358 monophyletic groups are identified, East and West of the Aegean. The East shows a
359 clear split between *L. pamphylica* and *L. trilineata*. In the West, Central Cyclades
360 populations branch first with all others monophyletic. These, in turn, form a southern

361 clade (Peloponnesos and Crete) and a northern one (mainland Greece, adjacent islands,
362 West Cyclades).

363 According to the ancestral-area reconstructions (Figure 4), using the topology
364 from SVDquartets, the ancestor of *trilineata+pamphylica* occurred in Anatolia
365 (probability 0.80), while the ancestor of the West lineage occurred in the Central
366 Cyclades islands (probability 0.76), revealing a dispersal event between the two regions.

367

368 **3.3. Mitochondrial gene-tree and divergence times**

369

370 The ML analysis ran with three partitions (per-codon position of *cytb*) and the
371 resulting mtDNA gene-tree supports four major clades including *L. pamphylica*, Central
372 Cyclades, East Aegean and West Aegean (Figure 3). The clade containing *L.*
373 *pamphylica* and Central Cyclades conflicts with the topologies supported by the
374 ddRADseq data, which place *L. pamphylica* sister to eastern populations and Central
375 Cyclades sister to western populations. The topology within the East mtDNA clade is
376 simple, with Lesvos Island forming a separate unit and populations from Turkey, East
377 Aegean islands and Thrace forming a monophyletic group (Figure 3). The West mtDNA
378 clade presents three monophyletic groups in polytomy: (a) west Peloponnesian
379 populations, (b) east Peloponnesian populations and Crete and (c) all other mainland
380 and island populations (Figure 3).

381 According to the estimated divergence times, the radiation within
382 *trilineata+pamphylica* occurred approximately 3.1 Mya (95% HPD intervals: 2.4-4.0
383 Mya) in the Late Pliocene (Figure 5). Similarly, the radiations of all other green-lizard
384 groups (*L. agilis* complex, *L. media* complex, *L. viridis/bilineata* complex), but also the
385 radiation of the eastern and western units of *trilineata+pamphylica*, took place roughly
386 at the same time (mean values from 3.0 to 3.5 Mya; combined intervals: 2.2-4.4 Mya).

387 4. DISCUSSION

388

389 4.1. Phylogenetic patterns and mitonuclear discordance

390

391 The discordant phylogenetic patterns derived from mtDNA and genomic markers fall
392 into three main categories. First, several relationships between major mtDNA lineages
393 of the *trilineata*+*pamphylica* clade are unresolved or even misleading. Collecting
394 thousands of independent loci and applying coalescence approaches that incorporate
395 incomplete lineage sorting assisted with their resolution. Second, using genome wide
396 SNPs allowed us to discover fine-scale genetic structure that was not apparent from
397 mtDNA alone. Finally, the use of independent nuclear markers facilitated the detection
398 of genetic admixture in several samples, which is linked to biogeographic mechanisms,
399 such as dispersals and secondary contacts.

400 STRUCTURE analyses clearly cluster Aegean *Lacerta* into Eastern and Western
401 groups, in full agreement with both coalescence and concatenated trees. In the East, *L.*
402 *pamphylica* and East Aegean *L. trilineata* are monophyletic. MtDNA phylogenies have
403 shown that *L. pamphylica* is nested within *L. trilineata*, but the clear *L. trilineata*
404 paraphyly was never supported by nodal support on mtDNA gene-trees or alternative
405 topology tests (Godinho, Crespo, Ferrand & Harris, 2005; Ahmadzadeh et al., 2013;
406 Sagonas et al., 2014; current study). The peculiar relationship of the easternmost *L.*
407 *pamphylica* to the Central Cyclades populations (Sagonas et al., 2014; current study), is
408 most probably artifactual, the result of attraction between these long mtDNA branches.
409 Genomic markers demonstrate that *L. trilineata* is paraphyletic in relation to *L.*
410 *pamphylica*, providing a clearer picture of the group's history but also reinforcing the
411 need for a general taxonomic re-evaluation. A thorough species-delimitation and
412 systematic review of this group is underway.

413 East *L. trilineata* populations form two groups, one corresponding to the island of
414 Lesbos and the other to all remaining populations (Figure 2b). One individual from the
415 neighbouring part of Turkey is admixed between the two. The unique genetic identity of
416 the samples from Lesbos is also demonstrated in the mtDNA tree (Sagonas et al., 2014;
417 current study). However, all phylogenomic trees show that these populations, although
418 genetically distinct, are nested within the east Aegean clade and do not represent an
419 ancient split.

420 Within the West Aegean, the Central Cyclades populations split very early in the
421 group's diversification history. The remaining western populations differentiate into a
422 southern and a northern assemblage, a pattern that is not clear in the mtDNA tree. The
423 situation in the south is very interesting: SVDquartets using individuals, SNAPP and

424 concatenated analyses return unresolved relationships among three southern lineages,
425 i.e. west Peloponnesos, east Peloponnesos and Crete, while the SVDquartets species-
426 tree and the mtDNA gene-tree favour the relationship between Crete and east
427 Peloponnesos, rendering the Peloponnesian populations paraphyletic (Figure 2 and 3).
428 STRUCTURE and DAPC do not differentiate the Peloponnesian populations into two
429 clusters but identify the Cretan ones as separate. Finally, an individual from the central
430 parts of Peloponnesos is nested in west Peloponnesos in the ddRAD concatenated tree
431 but in east Peloponnesos in the mtDNA tree (Figure 3). The biogeographic background
432 behind these complex patterns is not clear. Based on these results, Cretan populations
433 are closely related to the Peloponnesian ones and probably those of the southeastern
434 parts.

435 A similar interesting pattern is found within the north group. STRUCTURE and
436 DAPC cluster populations into three subgroups: West Cyclades, West mainland and
437 islands and East mainland and islands. While SVDquartets analysis of individuals and
438 concatenated ML show the West Cyclades phylogenetically close to the East mainland,
439 SNAPP and SVDquartets species-trees show unresolved relationships among the three
440 lineages. The distinction of mainland Balkan populations into West and East (of Pindos
441 Mt. range; Figure 1) is not clear in the mtDNA gene-tree but it is evident in the genomic
442 markers. However, it is also clear that the southwestern populations show proportions of
443 admixture with the east, implying genetic admixture between the two lineages (Figure 1
444 and 2).

445

446 **4.2. Synchronous *Lacerta* radiations in the Pliocene**

447

448 Our dating analysis included all green-lizard species and their internal mtDNA
449 diversity throughout their range, with the exception of *L. strigata* and *L. schreiberi*,
450 since we used all available *cytb* sequences, the most popular marker of choice for
451 lacertid phylogenies. According to our results, all *Lacerta* radiations seem to have
452 occurred during the same time (late Pliocene; Figure 5), in the same area (west Eurasia),
453 and may have been triggered by the same factor, most probably the Pliocene climate
454 transition (Salzmann et al., 2011). The Pliocene climatic fluctuations, coupled with the
455 geomorphology and geological history of Anatolia, were responsible for the radiation of
456 oriental green lizards into multiple lineages (Ahmadzadeh et al., 2013). *Lacerta media*
457 further diversified in the east during the same time interval, while the
458 *trilineata+pamphylica* group radiated in west Anatolia and the circum-Aegean region.

459 Our dating results agree almost perfectly with those from Ahmadzadeh et al.
460 (2013), but largely deviate from Sagonas et al. (2014), even though all three studies

461 included the same dataset (taxon-wise), type of marker (mtDNA) and calibration
462 strategy and implementation. However, when the latter study's dataset was re-analysed
463 here, in exactly the same manner, the published result could not be replicated (Appendix
464 S3). On the contrary, in all runs, the result always matched Ahmadzadeh et al. (2013)
465 and the present study. Even so, the more recent nodes were still slightly older
466 (Appendix S3). These slightly older dates were inferred when all sequences were
467 included in the re-analysis, but after representing each putative genetic cluster with only
468 one individual, the estimated times decreased and all three studies came to perfect
469 agreement with regard to the divergence-times (Appendix S3). It is clear that the
470 violation of the Yule speciation model, by including a great number of conspecific
471 sequences, led to an overestimation of divergence times for the MRCAs of the
472 respective entities. Additionally, the mean substitution rate for our *cytb* dataset was
473 estimated to be 0.0153 (95% HPD: 0.0123-0.0185), very close to the mean value
474 estimated for lacertids (0.0164; Carranza & Arnold, 2012), reinforcing the validity of
475 our dating results.

476

477 **4.3. Testing the biogeographic hypotheses**

478

479 The ancestral-area reconstruction shows that the ancestor of Aegean green lizards was
480 distributed in Anatolia while that of the populations west of the AB was distributed in
481 the Central Cyclades. Hence, the favoured biogeographic scenario includes a dispersal
482 event from Anatolia to the central Aegean islands and a second dispersal from the
483 islands to the southern part of the Balkan Peninsula (Figure 4). Consequently, the
484 biogeographic analysis supports the ISD hypothesis, according to which green lizards
485 crossed the Aegean and used the central Aegean islands as stepping-stones (Figure 4
486 and Appendix S1). Very different outcomes would have been expected if the other two
487 hypotheses were true. If the V scenario was favoured, then the ancestor of all studied
488 populations would be distributed in the entire Aegean area, on both sides of the AB (not
489 just Anatolia in the east), and the ancestor of the populations west of the AB would be
490 distributed in all or most of the regions defined west of the AB (not just the central
491 Aegean islands). Finally, if the OD hypothesis was favoured, then the ancestor of all
492 Aegean green lizards would be distributed in Anatolia but the ancestor of the
493 populations west of the AB would be distributed in at least the continental parts of the
494 Balkan Peninsula and possibly other regions too (not just the central Aegean islands
495 without the continental parts). The ISD hypothesis explains the outcome of all analyses
496 from both mtDNA and genome-wide markers and fits all present and published results,
497 with no need for assumptions of additional extinction events and secondary dispersals.

498 The two rejected hypotheses are in conflict with the phylogenomic and genetic-
499 structure results and/or demand multiple assumptions. The V hypothesis (Appendix S1),
500 favoured in Sagonas et al. (2014), follows the “Greek limbless skink paradigm”
501 (*Ophiomorus punctatissimus*), according to which vicariance is the mode of
502 diversification, as the formation of the AB fragments an old and wide distribution
503 (Poulakakis, Pakaki, Mylonas & Lymberakis, 2008). This hypothesis should be rejected
504 for the Aegean green lizards, not just because it is not supported by the biogeographical
505 analysis on genomic data, but also because the AB was completely formed several
506 millions of years before the estimated radiation time.

507 The OD hypothesis from Anatolia to the west after the formation of the AB
508 (Appendix S1), which is favoured by Ahmadzadeh et al. (2013), is more compatible
509 with the estimated divergence-times. This biogeographical pattern follows the “Snake-
510 eyed skink paradigm” (*Ablepharus kitaibelii*), a demonstrated case of dispersal from
511 Anatolia to the Balkan Peninsula around the AB (Skourtanioti et al., 2016). However,
512 the phylogenetic results for *Lacerta* largely deviate from those of the snake-eyed skink.
513 The latter phylogeny presents a branching pattern that follows the dispersal route from
514 the northeast to the south of the peninsula (Skourtanioti et al., 2016). Yet, the opposite
515 pattern is seen here for the Aegean *Lacerta*: high genetic diversity and structure is found
516 in the south and the branching in the tree follows a south to north route. Ahmadzadeh et
517 al. (2013) attribute this to an extinction event after the dispersal to the south of the
518 Balkans and a secondary dispersal from south to north. However, the major lineage of
519 the Central Cyclades was not represented in that study, hiding an important part of the
520 underlying history. Although the scenario of OD around the Aegean with a subsequent
521 extinction and a secondary northward dispersal cannot be definitively rejected, it is not
522 supported by the biogeographical analysis and it is much less parsimonious (Figure 4).

523

524 **4.4. Green lizards crossed the Aegean Barrier**

525

526 The emergence of the AB had a profound impact on the eastern Mediterranean
527 biodiversity. It is believed to be an impermeable barrier between the East and the West
528 and animals that have been found to have crossed it are considered as exceptions
529 (Lymberakis & Poulakakis, 2010). Most reptiles and amphibians that can be found on
530 both sides, having crossed over the AB instead of by-passing it in the north via overland
531 dispersal, have the bulk of their distribution on one side and appear on a single or few
532 locations on the other (e.g. one or a few islands). Usually these single crossings are very
533 recent, so that, besides rafting, human induced dispersals cannot be excluded
534 (Lymberakis & Poulakakis, 2010). There are only two cases of old dispersals of

535 herpetofauna species over the AB, but they too should be characterised as single
536 crossings. The dice snake *Natrix tessellata* mtDNA phylogeny presents an interesting
537 relationship between west Anatolia and Crete, dating back to the Plio-Pleistocene
538 boundary, so that a cross-barrier transmarine colonisation should be assumed (Kyriazi et
539 al., 2013). Second, the populations of the green toad *Bufo viridis* on one Cycladic island
540 (possibly more) belong to a distinct lineage that seems to be related to east Aegean
541 populations, a relationship that dates back to the early Pleistocene (Dufresnes et al.,
542 2018). Finally, other species are found on both sides of the AB as evident results of
543 anthropogenic dispersals (e.g. Kornilios et al., 2010).

544 In recent years, an emerging literature has demonstrated similar ancient cross-
545 barrier relationships for invertebrates (e.g. Kornilios, Poulakakis, Mylonas &
546 Vardinoyannis, 2009; Allegrucci, Trucchi & Sbordoni, 2011) that should also be
547 considered single crossings of the AB. Until now there has only been one clear case,
548 that of the trapdoor spider *Cyrtocarenum*, which has a large distribution on both sides of
549 the AB, a result of two synchronous eastward dispersals, via two different routes
550 (Kornilios et al., 2016). Interestingly the timing of those colonisations coincides with
551 the one found here for *Lacerta* and one of the routes through the Central Cyclades is the
552 same but on the opposite direction.

553 How did these recent and ancient single crossings and rare major expansions over
554 the AB happen? How did green lizards cross the Aegean? As already mentioned,
555 landbridges connecting the east and west parts of the Aegean have been depicted in
556 some, albeit few, palaeogeographic reconstructions (Creutzburg, 1963). If actual
557 landbridges existed during specific periods, these must have probably been very limited,
558 and they could have facilitated this dispersal. However, transmarine dispersal via rafting
559 combined with island-hopping is not an uncommon mode of long-distance dispersal in
560 reptiles, often favoured by winds, sea-currents and the influence of major rivers
561 (Hawlitschek, Ramírez Garrido & Glaw, 2017). While no information is available for
562 the palaeowinds and palaeocurrents of the region, several major rivers flow from west
563 Anatolia into the Aegean Sea that could promote westward dispersals. Moreover,
564 overseas dispersal would have been more possible during periods of glacial maxima as
565 early as in the late Pliocene, when the sea-level dropped dramatically expanding land
566 surfaces and reducing the distances between islands and lands (Van Andel &
567 Shackleton, 1982).

568

569 **4.5. Conclusions and historical biogeography of Aegean green lizards**

570

571 Our phylogenomic, biogeographic and mtDNA gene-tree analyses, together with the
572 estimated divergence-times, strongly support the Island Stepping-stone Dispersal
573 scenario. Green lizards offer a rare paradigm of diversification in the Aegean, where
574 populations largely expanded their geographical distribution and crossed the Aegean
575 Barrier by using the central Aegean islands as stepping stones. As already mentioned,
576 green lizards dispersed from Anatolia to the central Aegean islands by either using
577 actual landbridges or via rafting combined with island-hopping, if there were no land
578 connections at that time.

579 Our estimated divergence times show that the radiation of Aegean green lizards
580 (including the aforementioned dispersal over the AB) occurred sometime between 4.0
581 and 2.4 Ma (mean value: 3.1 Ma) (Figure 5). This time-period corresponds very well to
582 the Late Pliocene (Piacenzian: 3.6-2.6 Ma). During the early Pliocene, the central
583 Aegean islands formed a united landmass connected to the mainland; this connection
584 was disrupted during the late Pliocene and was never re-established (Anastasakis et al.,
585 2006). Hence, when green lizards dispersed to the central Cycladic landmass, the latter
586 was or was not connected to the mainland, depending on the exact time this
587 phylogenetic event happened (sometime between 4.0 and 2.4 Ma, according to the
588 molecular clock results) and the exact time this land connection was disrupted
589 (sometime during the period from early to late Pliocene). In this sense, and according to
590 our biogeographical analysis, green lizards further dispersed to the southern Balkan
591 Peninsula from the central Aegean island-mass, following either an overland or an
592 overseas dispersal mode. The opposite pattern of reptiles dispersing to the central
593 Aegean islands from the west (Balkan Peninsula) and then being isolated there is not at
594 all uncommon. In fact, in several cases, the phylogenetic split between west mainland
595 and central Aegean clades is estimated to have happened in the same time as for green
596 lizards, which is attributed to the aforementioned land connection and subsequent
597 disconnection (Ursenbacher et al., 2008; Kyriazi et al., 2013; Kornilios et al., 2014).
598 The opposite pattern of colonisation found here for *Lacerta* is unique among
599 vertebrates, but is dated during the same time.

600 Ahmadzadeh et al. (2013) conclude that also during the late Pliocene, climatic
601 factors coupled with the geology of Anatolia differentiated oriental green lizards,
602 including those of the studied group into two ancestral units. Consequently, during a
603 relatively short period, sometime during the late Pliocene, an ancestor spread westwards
604 from Anatolia to the central Aegean islands and from there to the southern Balkan
605 Peninsula, while the Anatolian populations further diversified because of climatic
606 factors. At the end of the Pliocene, this rapid radiation led to four ancestral lineages in

607 the area, now identified as the four major clades of the mtDNA and phylogenomic trees:
608 *L. pamphylica*, East *L. trilineata*, Central Cyclades *L. trilineata* and West *L. trilineata*.

609 Later on, during the late Pleistocene, Crete was colonised from the southeastern
610 parts of the Peloponnese (Figure 4 and 5). At that time Crete had no connections with
611 the mainland (Dermitzakis, 1990), which means this colonisation probably also
612 happened overseas during times of lower sea-level, with Kythera and Antikythera
613 islands acting as stepping stones (Figure 1). In fact, green-lizards from Crete and
614 Kythera form a single mtDNA clade (Sagonas et al., 2014). The situation within
615 Peloponnesos implies an old occurrence and isolation of *Lacerta*, with the existence of
616 two lineages that might even be paraphyletic. Peloponnesos, the southernmost tip of the
617 Balkan Peninsula, is an important biodiversity hotspot, as a result of its complicated
618 geological history and its role as a refugial area (Thanou, Giokas & Kornilios, 2014 and
619 references therein). Additionally, the West Cyclades do not host the Central Cyclades
620 lineage: they were colonised overseas from the east parts of mainland Greece in the late
621 Pleistocene, with a mechanism similar to that of Crete. Finally, the distinction of Greek
622 mainland populations, west and east of the Pindos mountain ridge (Figure 1b),
623 highlights the biogeographical role of this formation, as shown in other studies of
624 reptiles (e.g. Thanou et al., 2014).

625

627 **ACKNOWLEDGMENTS**

628 This project has received funding from the European Union’s Horizon 2020 research
629 and innovation programme under the Marie Skłodowska-Curie grant agreement No
630 656006 (Project Acronym: CoPhyMed). This work used the Vincent J. Coates
631 Genomics Sequencing Laboratory at UC Berkeley, supported by NIH S10 OD018174
632 Instrumentation Grant. We are grateful to Kevin Epperly for his help with lab-work and
633 J. Howlett for the linguistic support of the text. We declare that we have no conflict of
634 interest.

635

636 **Data Accessibility**

637 Input files for the analyses based on ddRAD data are stored in Dryad
638 (doi:10.5061/dryad.15d8dq8). Newly generated mtDNA sequences have been deposited
639 in GenBank (Accession Numbers: MK330103 – MK330131).

640

641 **Supporting information**

642 Additional Supporting Information may be found in the online version of this article:

643

644 Appendix S1 The three biogeographic hypotheses discussed in the manuscript.

645 Appendix S2 Summary of the iPyRAD pipeline.

646 Appendix S3 Re-visiting the molecular-dating analysis of Sagonas et al. (2014).

648 **REFERENCES**

- 649 Ahmadzadeh, F., Carretero, M. A., Harris, D. J., Perera, A., & Böhme, W. (2012). A
650 molecular phylogeny of eastern group of ocellated lizard genus *Timon* (Sauria:
651 Lacertidae) based on mitochondrial and nuclear DNA sequences. *Amphibia-
652 Reptilia*, 33, 1–10.
- 653 Ahmadzadeh, F., Flecks, M., Rödder, D., Böhme, W., Ilgaz, Ç., Harris, J.D., ...
654 Carretero, M.A. (2013). Multiple dispersal out of Anatolia: biogeography and
655 evolution of oriental green lizards. *Biological Journal of the Linnean Society*, 110,
656 398–408.
- 657 Allegrucci, G., Trucchi, E., & Sbordoni, V. (2011). Time and mode of species
658 diversification in *Dolichopoda* cave crickets (Orthoptera, Rhaphidophoridae).
659 *Molecular Phylogenetics and Evolution*, 60, 108–121.
- 660 Anastasakis, G., Piper, D.J.W., Dermitzakis, M.D., & Karakitsios, V. (2006). Upper
661 Cenozoic stratigraphy and paleogeographic evolution of Myrtoon and adjacent
662 basins, Aegean Sea, Greece. *Marine and Petroleum Geology*, 23, 353–369.
- 663 Böhme, M.U., Schneeweiss, N., Fritz, U., Schlegel, M., & Berendonk, T.U. (2006).
664 Small edge populations at risk: genetic diversity of the green lizard (*Lacerta viridis
665 viridis*) in Germany and implications for conservation management. *Conservation
666 Genetics*, 8, 555–563.
- 667 Bouckaert, R., Heled, J., Kühnert, D., Vaughan, T., Wu, C.H., Xie, D., ... Drummond,
668 A.J. (2014). Beast 2: A software platform for Bayesian evolutionary analysis.
669 *PLoS Computational Biology*, 10, e1003537.
- 670 Bryant, D., Bouckaert, R., Felsenstein, J., Rosenberg, N.A., & RoyChoudhury, A.
671 (2012). Inferring species trees directly from biallelic genetic markers: bypassing
672 gene trees in a full coalescent analysis. *Molecular Biology and Evolution*, 29,
673 1917–1932.
- 674 Burbrink, F.T., Lawson, R. & Slowinski, J.B. (2000). Mitochondrial DNA
675 phylogeography of the polytypic North American rat snake (*Elaphe obsoleta*): A
676 critique of the subspecies concept. *Evolution*, 54, 2107–2118.
- 677 Busack, S. D., & Lawson, R. (2008). Morphological, mitochondrial DNA and allozyme
678 evolution in representative amphibians and reptiles inhabiting each side of the
679 Strait of Gibraltar. *Biological Journal of the Linnean Society*, 94, 445–461.

- 680 Camargo, A., Sinervo, B., & Sites, J.W.Jr. (2010). Lizards as model organisms for
681 linking phylogeographic and speciation studies. *Molecular Ecology*, 19, 3250–70.
- 682 Carranza, S., & Arnold, E.N. (2012). A review of the geckos of the genus
683 *Hemidactylus* (Squamata: Gekkonidae) from Oman based on morphology,
684 mitochondrial and nuclear data, with descriptions of eight new species. *Zootaxa*,
685 3378, 1–95.
- 686 Carranza, S., Arnold, E. N., & Amat, F. (2004). DNA phylogeny of *Lacerta*
687 (*Iberolacerta*) and other lacertine lizards (Reptilia: Lacertidae): Did competition
688 cause long-term mountain restriction? *Systematics and Biodiversity*, 2, 57-77.
- 689 Chernomor, O., von Haeseler, A., & Minh, B.Q. (2016). Terrace aware data structure
690 for phylogenomic inference from supermatrices. *Systematics Biology*, 65, 997–
691 1008.
- 692 Chifman, J., & Kubatko, L., (2014). Quartet inference from SNP data under the
693 coalescent model. *Bioinformatics*, 30, 3317–3324.
- 694 Creutzburg, N. (1963). Paleogeographic evolution of Crete from Miocene till our days.
695 *Cretan Annales*, 15/16, 336–342. (in Greek).
- 696 Dermitzakis, M.D. (1990). Paleogeography, geodynamic processes and event
697 stratigraphy during the late Cenozoic of the Aegean area *Accademia Nazionale*
698 *dei Lincei*, 85, 263–288.
- 699 Drummond, A.J., Suchard, M.A., Xie, D., & Rambaut, A. (2012). Bayesian
700 phylogenetics with BEAUti and the BEAST 1.7. *Molecular Biology and*
701 *Evolution*, 29, 1969–1973.
- 702 Dufresnes, C., Lymberakis, P., Kornilios, P., Savary, R., Perrin, N. & Stöck, M. (2018).
703 Phylogeography of Aegean green toads (*Bufo viridis* subgroup): continental
704 hybrid swarm vs. insular diversification with discovery of a new island endemic.
705 *BMC Evolutionary Biology*, 18, 67.
- 706 Eaton, D.A.R. (2014). PyRAD: assembly of de novo RADseq loci for phylogenetic
707 analyses. *Bioinformatics*, 30, 1844–1849.
- 708 Edgar, R.C. (2004). MUSCLE: multiple sequence alignment with high accuracy and
709 high throughput. *Nucleic Acids Research*, 32, 1792–1797.

- 710 Evanno, G., Regnaut, S., & Goudet, J. (2005). Detecting the number of clusters of
711 individuals using the software STRUCTURE: a simulation study. *Molecular*
712 *Ecology*, 14, 2611–2620.
- 713 Falush, D., Stephens, M., & Pritchard, J. K. (2003). Inference of population structure:
714 Extensions to linked loci and correlated allele frequencies. *Genetics*, 164, 1567–
715 1587.
- 716 Godinho, R., Crespo, E.G., Ferrand, N., & Harris, D.J. (2005). Phylogeny and evolution
717 of the green lizards, *Lacerta* spp. (Squamata: Lacertidae) based on mitochondrial
718 and nuclear DNA sequences. *Amphibia-Reptilia*, 26, 271–285.
- 719 Guindon, S., Dufayard, J.F., Lefort, V., Anisimova, M., Hordijk, W., & Gascuel, O.
720 (2010). New algorithms and methods to estimate maximum-likelihood
721 phylogenies: assessing the performance of PhyML 3.0. *Systematic Biology*, 59,
722 307–321.
- 723 Hawlitschek, O., Ramírez Garrido, S., & Glaw, F. (2017). How marine currents
724 influenced the widespread natural overseas dispersal of reptiles in the Western
725 Indian Ocean region. *Journal of Biogeography*, 44, 1435–1440.
- 726 Jombart, T. (2008). adegenet: A R package for the multivariate analysis of genetic
727 markers. *Bioinformatics*, 24, 1403–1405.
- 728 Jombart, T., Devillard, S., & Balloux, F. (2010). Discriminant analysis of principal
729 components: A new method for the analysis of genetically structured populations.
730 *BMC Genetics*, 11, 94.
- 731 Kapli, P., Lutteropp, S., Zhang, J., Kobert, K., Pavlidis, P., Stamatakis, A., & Flouri, T.
732 (2017). Multi-rate Poisson tree processes for single-locus species delimitation
733 under maximum likelihood and Markov chain Monte Carlo. *Bioinformatics*, 33,
734 1630–1638.
- 735 Kopelman, N.M., Mayzel, J., Jakobsson, M., Rosenberg, N.A., & Mayrose, I. (2015).
736 Clumpak: a program for identifying clustering modes and packaging population
737 structure inferences across K. *Molecular Ecology Resources*, 15, 1179–1191.
- 738 Kornilios, P., Kyriazi, P., Poulakakis, N., Kumlutaş, Y., Ilgaz, Ç., Mylonas, M., &
739 Lymberakis, P. (2010). Phylogeography of the ocellated skink *Chalcides ocellatus*
740 (Squamata, Scincidae), with the use of mtDNA sequences: A hitch-hiker's guide to
741 the Mediterranean. *Molecular Phylogenetics and Evolution*, 54, 445–456.

- 742 Kornilios, P., Poulakakis, N., Mylonas, M., & Vardinoyannis, K. (2009). The phylogeny
743 and biogeography of the genus *Zonites* Montfort, 1810 (Gastropoda: Pulmonata):
744 preliminary evidence from mitochondrial data. *Journal of Molluscan Studies*, 75,
745 109–117.
- 746 Kornilios, P., Thanou, E., Kapli, P., Parmakelis, A., & Chatzaki, M. (2016). Peeking
747 through the trapdoor: historical biogeography of the Aegean endemic spider
748 *Cyrtocarenum* Ausserer, 1871 with an estimation of mtDNA substitution rates for
749 Mygalomorphae. *Molecular Phylogenetics and Evolution*, 98, 300–313.
- 750 Kornilios, P., E. Thanou, P. Lymberakis, R. Sindaco, C. Liuzzi & S. Giokas. (2013).
751 Mitochondrial phylogeography, intraspecific diversity and phenotypic
752 convergence in the four-lined snake (Reptilia, Squamata). *Zoologica Scripta*, 43,
753 149-160.
- 754 Kyriazi, P., Kornilios, P., Nagy, Z.T., Poulakakis, N., Kumlutaş, Y., Ilgaz, Ç., ...
755 Lymberakis, P. (2013). Comparative phylogeography reveals distinct colonization
756 patterns of Cretan snakes. *Journal of Biogeography*, 40, 1143–1155.
- 757 Le Pinchon, X., & Angelier, J. (1981). The Hellenic arc and trench system: a key to the
758 neotectonic evolution of the eastern Mediterranean area. *Philosophical
759 Transactions of the Royal Society of London*, 300, 357–372.
- 760 Lymberakis, P., & Poulakakis, N. (2010). Three continents claiming an archipelago: the
761 evolution of Aegean's Herpetofaunal diversity. *Diversity*, 2, 233–255.
- 762 Marzahn, E., Mayer, W., Joger, U., Ilgaz, Ç., Jablonski, D., Kindler, C., Kumlutaş, Y.,
763 Nistri, A., Schneeweiss, N., Vamberger, M., Žagar, A., & Fritz, U. (2016).
764 Phylogeography of the *L. viridis* complex: mitochondrial and nuclear markers
765 provide taxonomic insights. *Journal of Zoological Systematics and Evolutionary
766 Research*, 54, 85–105.
- 767 Miller, M.A., Pfeiffer, W., & Schwartz, T. (2010). Creating the CIPRES Science
768 Gateway for inference of large phylogenetic trees. *Proceedings of the Gateway
769 Computing Environments Workshop (GCE)*, New Orleans, LA, 1–8.
- 770 Minh, B.Q., Nguyen, M.A.T., & von Haeseler, A. (2013). Ultrafast approximation for
771 phylogenetic bootstrap. *Molecular Biology and Evolution*, 30, 1188–1195.

- 772 Nguyen, L.-T., Schmidt, H.A., von Haeseler, A., & Minh, B.Q. (2015). IQTREE: A fast
773 and effective stochastic algorithm for estimating maximum likelihood phylogenies.
774 *Molecular Biology and Evolution*, 32, 268–274.
- 775 Paulo, O. S., Pinheiro, J., Miraldo, A., Bruford, M. W., Jordan, W. C., & Nichols, R. A.
776 (2008). The role of vicariance vs. dispersal in shaping genetic patterns in ocellated
777 lizard species in the western Mediterranean. *Molecular Ecology*, 17, 1535–1551.
- 778 Pavlicev, M., Mayer, W. (2009). Fast radiation of the subfamily Lacertinae (Reptilia:
779 Lacertidae): History or methodical artefact? *Molecular Phylogenetics and*
780 *Evolution*, 52, 727-734.
- 781 Peterson, B.K., Weber, J.N., Kay, E.H., Fisher, H.S., & Hoekstra, H.E. (2012). Double
782 digest RADseq: an inexpensive method for de novo SNP discovery and
783 genotyping in model and non-model species. *PLoS ONE*, 7, e37135.
- 784 Poulakakis, N., Lymberakis, P., Antoniou, A., Chalkia, D., Zouros, E., Mylonas, M., &
785 Valakos, E. (2003). Molecular phylogeny and biogeography of the wall-lizard
786 *Podarcis erhardii* (Squamata: Lacertidae). *Molecular Phylogenetics and*
787 *Evolution*, 28, 38–46.
- 788 Poulakakis, N., Pakaki, V., Mylonas, M., & Lymberakis, P. (2008). Molecular
789 phylogeny of the Greek legless skink *Ophiomorus punctatissimus* (Squamata:
790 Scincidae): The impact of the Mid-Aegean trench in its phylogeography.
791 *Molecular Phylogenetics and Evolution*, 47, 396–402.
- 792 Pritchard, J.K., Stephens, M., & Donnelly, P (2000). Inference of population structure
793 using multilocus genotype data. *Genetics*, 155, 945–959.
- 794 Rambaut, A., & Drummond, A.J. (2007). Tracer v1.5. Available from
795 [http://tree.bio.ed.ac.uk/ software/tracer/](http://tree.bio.ed.ac.uk/software/tracer/).
- 796 Rognes, T., Flouri, T., Nichols, B., Quince, C., & Mahé, F. (2016). A versatile open
797 source tool for metagenomics. *Peerj*, 4, e2584.
- 798 Sagonas, K., Poulakakis, N., Lymberakis, P., Parmakelis, A., Pafilis, P., & Valakos,
799 E.D. (2014). Molecular systematics and historical biogeography of the green
800 lizards (*Lacerta*) in Greece: Insights from mitochondrial and nuclear DNA.
801 *Molecular Phylogenetics and Evolution*, 76, 144–154.

- 802 Salzman, U., Williams, M., Haywood, A.M., Johnson, A.L.A., Kender, S., &
803 Zalasiewicz, J. (2011). Climate and environment of a Pliocene warm world.
804 *Palaeogeography, Palaeoclimatology, Palaeoecology*, 309, 1–8.
- 805 Skourtanioti, E., Kapli, P., Ilgaz, Ç., Kumlutaş, Y., Avcı, A., Ahmadzadeh, F., ...
806 Poulakakis, N. (2016). A reinvestigation of phylogeny and divergence times of the
807 *Ablepharus kitaibelii* species complex (Sauria, Scincidae) based on MtDNA and
808 NuDNA genes. *Molecular Phylogenetics and Evolution*, 103, 199–214.
- 809 Swofford, D.L. (2003). *PAUP*: Phylogenetic Analysis Using Parsimony, Version 4.0*
810 *b10*. Sinauer Associates, Sunderland.
- 811 Thanou, E., Giokas, S., & Kornilios, P. (2014). Phylogeography and genetic structure of
812 the slow worms *Anguis cephallonica* and *Anguis graeca* (Squamata: Anguidae)
813 from the southern Balkan Peninsula. *Amphibia – Reptilia*, 35, 263–269.
- 814 Ursenbacher, S., Schweiger, S., Tomović, L., Crnobrnja-Isailović, J., Fumagalli, L. &
815 Mayer, W. (2008). Molecular phylogeography of the nose-horned viper (*Vipera*
816 *ammodytes*): evidence for high genetic diversity and multiple refugia in the Balkan
817 peninsula. *Molecular Phylogenetics and Evolution*, 46, 1116–1128.
- 818 Van Andel, T., & Shackleton, J. (1982). Late Paleolithic and Mesolithic Coastlines of
819 Greece and the Aegean. *Journal of Field Archaeology*, 9(4), 445-454.
- 820 Yu, Y., Harris, A.J., Blair, C., & He, X.J. (2015). RASP (Reconstruct Ancestral State in
821 Phylogenies): a tool for historical biogeography. *Molecular Phylogenetics and*
822 *Evolution*, 87, 46–49.

824 **Biosketch:**

825 **Panagiotis Kornilios** is a postdoctoral fellow working on animal phylogenetics,
826 phylogeography, molecular ecology and evolution. This work is part of a Marie Curie-
827 Skłodowska Global Fellowship awarded to PK and hosted by the Leaché Lab
828 (University of Washington, Seattle, USA) and the Carranza Lab (IBE, Barcelona,
829 Spain). PK's current work focuses on the application of genome-targeted benchwork
830 and analytical methods on comparative phylogeography. The authors have a long-
831 lasting collaboration in phylogeography and phylogenetics of animal taxa, especially
832 reptiles, from the eastern Mediterranean.

833

834 **Author contributions:** P.K. conceived the idea; P.K., E.T. and A.L. designed the work;
835 P.K., E.T., P.L. Ç.I., and Y.K. collected and/or contributed specimens; P.K. and E.T.
836 carried out laboratory work and analyses; P.K. led the writing and all authors were
837 involved in the writing process.

838 **Table 1.**

839 Information regarding the samples analysed in the current study. The first column (left)
 840 shows the working codes of the samples and, in some cases, the GenBank Accession
 841 Numbers of the respective sequences that we used as working codes. The first 34
 842 samples (bold) are the ones included in the ddRAD analyses. Other information
 843 includes the species names and sampling localities (with regions and country) of the
 844 analysed specimens. For the ones retrieved from GenBank, the source (literature) is
 845 reported, instead of the sampling locality. NHMC = Natural History Museum of Crete.
 846 Accession numbers of sequence data that were generated here or retrieved from
 847 GenBank are shown in the last column of the table. Input files for the analyses based on
 848 ddRAD (double-digest restriction-site-associated DNA) data are stored in Dryad
 849 (doi:10.5061/dryad.15d8dq8).

850

851

Working Code	Species	Locality, Region / Source (Literature)	GenBank Accession Numbers Cytochrome b
LT391	<i>L. trilineata</i>	Skyros isl., Greece	MK330107
LT393	<i>L. trilineata</i>	Skyros isl., Greece	MK330108
LT394	<i>L. trilineata</i>	Milos isl., Greece	MK330112
LT402	<i>L. trilineata</i>	Kimolos isl., Greece	MK330113
LT441	<i>L. trilineata</i>	Crete isl., Greece	MK330117
LT446	<i>L. trilineata</i>	Crete isl., Greece	MK330118
LT371	<i>L. trilineata</i>	Naxos isl., Greece	MK330119
NHMC80.3.61.76	<i>L. trilineata</i>	Serifos isl., Greece	MK330111
LT416	<i>L. trilineata</i>	Tinos isl., Greece	MK330121
LT375	<i>L. trilineata</i>	Naxos isl., Greece	MK330120
LT353	<i>L. trilineata</i>	Kaiafas, Peloponnesos, Greece	MK330114
LT360	<i>L. trilineata</i>	Selinountas, Peloponnesos, Greece	MK330103
LT377	<i>L. trilineata</i>	Argolis, Peloponnesos, Greece	MK330115
LT378	<i>L. trilineata</i>	Argolis, Peloponnesos, Greece	MK330104
LT345	<i>L. trilineata</i>	Feneos, Peloponnesos, Greece	MK330116
LT382	<i>L. trilineata</i>	Evvoia, Greece	MK330109
LT469	<i>L. trilineata</i>	Aitolokarnania, Greece	MK330106
NHMC80.3.60.276	<i>L. trilineata</i>	Rhodos isl., Greece	MK330127
NHMC80.3.60.277	<i>L. trilineata</i>	Rhodos isl., Greece	MK330128
NHMC80.3.60.316	<i>L. trilineata</i>	Xanthi, Greece	-
NHMC80.3.60.217	<i>L. trilineata</i>	Dodoni, Greece	MK330105
NHMC80.3.60.418	<i>L. trilineata</i>	Kerkyra isl., Greece	MK330110
NHMC80.3.60.419	<i>L. trilineata</i>	Kerkyra isl., Greece	-
NHMC80.3.60.185	<i>L. trilineata</i>	Lesvos isl., Greece	MK330122
NHMC80.3.60.186	<i>L. trilineata</i>	Lesvos isl., Greece	-
LT408	<i>L. trilineata</i>	Samos isl., Greece	MK330123
LT2	<i>L. trilineata</i>	Kertil, Balıkesir, Turkey	MK330129
LT3	<i>L. trilineata</i>	Evciler, Bayramiç, Çanakkale, Turkey	MK330131
LT6	<i>L. trilineata</i>	Çığı village, Başmakçı, Afyon, Turkey	MK330130
LT8	<i>L. trilineata</i>	Koçarlı, Aydın, Turkey	MK330124
LP2	<i>L. pamphylica</i>	Akseki, Antalya, Turkey	MK330125
LP3	<i>L. pamphylica</i>	Karakışla, Akseki, Antalya, Turkey	MK330126
LV480	<i>L. viridis</i>	Pertouli, Greece	-
NHMC80.3.60.413	<i>L. viridis</i>	Evros, Greece	-
KC897016	<i>L. trilineata</i>	Ahmadzadeh et al. (2013)	KC897016
KC897015	<i>L. trilineata</i>	Ahmadzadeh et al. (2013)	KC897015

KC897014	<i>L. trilineata</i>	Ahmadzadeh et al. (2013)	KC897014
KC897017	<i>L. trilineata</i>	Ahmadzadeh et al. (2013)	KC897017
KC897018	<i>L. trilineata</i>	Ahmadzadeh et al. (2013)	KC897018
KC897021	<i>L. trilineata</i>	Ahmadzadeh et al. (2013)	KC897021
KC897020	<i>L. trilineata</i>	Ahmadzadeh et al. (2013)	KC897020
KC897019	<i>L. trilineata</i>	Ahmadzadeh et al. (2013)	KC897019
LN835029	<i>L. trilineata</i>	Marzahn et al. (2016)	LN835029
LN835028	<i>L. trilineata</i>	Marzahn et al. (2016)	LN835028
KC897013	<i>L. pamphylica</i>	Ahmadzadeh et al. (2013)	KC897013
LN835022	<i>L. pamphylica</i>	Marzahn et al. (2016)	LN835022
KC896975	<i>L. media</i>	Ahmadzadeh et al. (2013)	KC896975
KC897005	<i>L. media</i>	Ahmadzadeh et al. (2013)	KC897005
KC896982	<i>L. media</i>	Ahmadzadeh et al. (2013)	KC896982
KC896988	<i>L. media</i>	Ahmadzadeh et al. (2013)	KC896988
LN835021	<i>L. media</i>	Marzahn et al. (2016)	LN835021
GQ142118	<i>L. agilis</i>	Pavlicev and Mayer (2009)	GQ142118
LN834626	<i>L. bilineata</i>	Marzahn et al. (2016)	LN834626
LN834643	<i>L. bilineata</i>	Marzahn et al. (2016)	LN834643
LN834669	<i>L. bilineata</i>	Marzahn et al. (2016)	LN834669
LN834710	<i>L. bilineata</i>	Marzahn et al. (2016)	LN834710
LN834705	<i>L. bilineata</i>	Marzahn et al. (2016)	LN834705
LN834743	<i>L. viridis</i>	Marzahn et al. (2016)	LN834743
LN834723	<i>L. viridis</i>	Marzahn et al. (2016)	LN834723
LN834769	<i>L. viridis</i>	Marzahn et al. (2016)	LN834769
LN834818	<i>L. viridis</i>	Marzahn et al. (2016)	LN834818
LN835024	<i>L. strigata</i>	Marzahn et al. (2016)	LN835024
LN835023	<i>L. schreiberi</i>	Marzahn et al. (2016)	LN835023
AY616290	<i>L. agilis</i>	Kalyabina-Hauf and Ananjeva (2004). Direct submission	AY616290
AY616335	<i>L. agilis</i>	Kalyabina-Hauf and Ananjeva (2004). Direct submission	AY616335
KC665499	<i>L. agilis</i>	Andres,C. (2013) Direct submission	KC665499
LN835020	<i>L. agilis</i>	Marzahn et al. (2016)	LN835020
AY616263	<i>L. agilis</i>	Kalyabina-Hauf and Ananjeva (2004). Direct submission	AY616263
KC665498	<i>L. agilis</i>	Andres,C. (2013) Direct submission	KC665498
AY616305	<i>L. agilis</i>	Kalyabina-Hauf and Ananjeva (2004). Direct submission	AY616305
AY616241	<i>L. agilis</i>	Kalyabina-Hauf and Ananjeva (2004). Direct submission	AY616241
KC665477	<i>L. agilis</i>	Andres,C. (2013) Direct submission	KC665477
KC665471	<i>L. agilis</i>	Andres,C. (2013) Direct submission	KC665471
DQ902143	<i>Timon tangitanus</i>	Busack and Lawson (2008)	DQ902143
AF378967	<i>Timon pater</i>	Paulo et al. (2008)	AF378967
GQ142119	<i>Timon nevadensis</i>	Pavlicev and Mayer (2009)	GQ142119
DQ902142	<i>Timon lepidus</i>	Busack and Lawson (2008)	DQ902142
JQ425836	<i>Timon kurdistanicus</i>	Ahmadzadeh, F., Carretero, M. A., Harris, D. J., Perera, A., & Böhme, W. (2012)	JQ425836
AY151838	<i>Gallotia stehlini</i>	Carranza, S., Arnold, E. N., & Amat, F. (2004)	AY151838
AY151836	<i>Gallotia atlantica</i>	Carranza, S., Arnold, E. N., & Amat, F. (2004)	AY151836
AY151844	<i>Gallotia intermedia</i>	Carranza, S., Arnold, E. N., & Amat, F. (2004)	AY151844
AM489592	<i>Gallotia galloti</i>	Klassert,T.E., Suarez,N.M., Almeida,T., Lopez,M., Pestano,J.J. and Hernandez,M. (2007) Direct submission	AM489592
AY154903	<i>Gallotia caesaris</i>	Carranza, S., Arnold, E. N., & Amat, F. (2004)	AY154903
AY154902	<i>Gallotia caesaris</i>	Carranza, S., Arnold, E. N., & Amat, F. (2004)	AY154902

853 **Table 2.**

854 Summary of the ddRAD (double-digest restriction-site-associated DNA) data matrices,
 855 as resulted from the iPyRAD pipeline. This includes information on the number of
 856 prefiltered and filtered loci, the total number of base pairs, and the number of Single
 857 Nucleotide Polymorphisms (SNPs), unlinked uSNPs and biallelic uSNPs. This
 858 information is presented for three different datasets built with different percentages of
 859 missing data, expressed as % of individuals for a given locus: D0 (0% missing data, i.e.
 860 all loci present for all samples), D10 (10% missing data, all loci present for at least 90%
 861 of the samples) and D25 (25% missing data, all loci present for at least 90% of the
 862 samples). Dataset D25 also included the outgroup *Lacerta viridis*. These datasets were
 863 used in different downstream analyses: DAPC = Discriminant Analysis of Principal
 864 Components implemented in the R package ADEGENET; STRUCTURE = Bayesian
 865 clustering analysis; SNAPP = SNP and AFLP Package for Phylogenetic analysis
 866 implemented in BEAST2 (Bayesian Evolutionary Analysis Sampling Trees);
 867 SVDquartets implemented in PAUP* (Phylogenetic Analysis Using Parsimony);
 868 Concatenation = maximum likelihood analysis in IQ-TREE. Next to each analysis, we
 869 report which type of dataset was used: uSNPs, biallelic uSNPs, ddRAD (the entire
 870 sequence of the ddRAD loci).

871

Dataset name		D0	D10	D25-outgroup
iPyRAD parameters	Minimum % of individuals for a given locus	100	90	75
Results Statistics	Number of prefiltered loci	67,999		73,575
	Number of filtered loci	599	5,944	11,620
	Total number of base pairs	24,036	238,331	466,138
	Number of SNPs	1,141	10,993	25,715
	Number of uSNPs	470	4,767	9,873
	Number of biallelic uSNPs	-	2,199	-
Final Analyses	DAPC	uSNPS		
	STRUCTURE	uSNPS		
	SNAPP	uSNPS biallelic		
	SVDquartets	uSNPS		
	Concatenation	ddRAD		

872

873

874 **FIGURE 1.**

875 The Aegean region, situated in the east Mediterranean (see inset at the lower right of the
876 figure) and the geographical distributions of the study taxa *L. trilineata* and *L.*
877 *pamphylica*. The sampling localities are shown as black dots, with the sample codes
878 next to them. These sampling codes are also given in Table 1, together with other
879 information on the analysed material. The ddRAD (double-digest restriction-site-
880 associated DNA) assemblies included a total of 34 samples, with two *L. viridis*
881 individuals used as outgroups (Table 1). The mitochondrial DNA maximum likelihood
882 phylogeny was built on 47 complete cytochrome *b* sequences (41 ingroup), while 31
883 additional sequences were used in the final molecular clock analysis (Table 1). (b) The
884 sampling localities of the present study: small circles/squares = mitochondrial DNA
885 (mtDNA) data, large circles/squares = mtDNA and ddRAD data (double-digest
886 restriction-site-associated DNA). Colour of the circles corresponds to the identified
887 clusters from the genetic structure analyses, i.e. DAPC (Discriminant Analysis of
888 Principal Components implemented in the R package ADEGENET) and the hierarchical
889 Bayesian population clustering with STRUCTURE), and the identified genetic lineages
890 from SVDquartets, implemented in PAUP* (Phylogenetic Analysis Using Parsimony)
891 and SNAPP (SNP and AFLP Package for Phylogenetic analysis), implemented in
892 BEAST2 (Bayesian Evolutionary Analysis Sampling Trees), as shown in Figure 2. In
893 three cases, admixed populations, as derived from STRUCTURE, are shown as pies,
894 with different colours representing the admixture proportion of each cluster. In the same
895 Figure 1b, the seven geographical areas that were defined for the ancestral-area
896 reconstruction analysis are also shown, with different colours corresponding to those of
897 Figure 4. Names of islands and other geographic elements, mentioned in the manuscript,
898 are also presented.

899

900 **FIGURE 2.**

901 Species-tree and genetic clustering results, using the unlinked SNPs dataset (unlinked
902 Single Nucleotide Polymorphisms). (a) Tree derived from the Bayesian coalescence
903 analysis of SNAPP (SNP and AFLP Package for Phylogenetic analysis) implemented in
904 BEAST2 (Bayesian Evolutionary Analysis Sampling Trees). Values on nodes represent
905 statistical support (SNAPP posterior probability / Bootstrap values from SVDquartets
906 species-tree analysis) with filled circles representing full support (1.0 and 100). (b) The
907 results from the Discriminant Analysis of Principal Components (DAPC) (optimal $K=8$
908 and number of PCA=3) implemented in the R package ADEGENET. (c) The results
909 from the hierarchical Bayesian population clustering with STRUCTURE, shown next to
910 the corresponding clades of the species-tree. Horizontal bars represent individuals with

911 the colour of each one representing the proportion of that individual's membership in
 912 each cluster. From right to left: all populations (optimal $K=2$); populations from east
 913 and west of the Aegean Barrier (optimal $K=3$, in both cases); populations from the north
 914 and south (optimal $K=3$ and $K=2$, respectively). The colours of each STRUCTURE
 915 cluster correspond to those of the clusters in DAPC (Figure 2b) and the clades of the
 916 species-tree (Figure 2a). They also correspond to the colours of the circles/pies that
 917 represent sampling localities in Figure 1.

918

919 **FIGURE 3.**

920 Left: Results from the phylogenomic analyses using individuals as terminal branches:
 921 Maximum likelihood (ML) tree on the concatenated ddRAD (double-digest restriction-
 922 site-associated DNA) loci from IQ-tree and SVDquartets, implemented in PAUP*
 923 (Phylogenetic Analysis Using Parsimony) on the unlinked SNPs (Single Nucleotide
 924 Polymorphisms). The tree presented is the one from the concatenated ddRAD loci with
 925 the statistical support on the nodes from both analyses (SH-aLRT, i.e. Shimodaira–
 926 Hasegawa approximate Likelihood Ratio Test, from IQ-tree / ultrafast bootstraps from
 927 IQ-tree / bootstrap values from SVDquartets). Filled circles indicate full support. Right:
 928 the ML tree from IQ-tree based on the mitochondrial DNA. Filled circles on nodes
 929 indicate full support (1.0 and 100) while open circles represent nodes with weaker
 930 support (SH-aLRT / ultrafast bootstraps / standard bootstraps). Dashed lines highlight
 931 specimens with interesting phylogenetic placements discussed in the text. Sample codes
 932 for terminals are provided in Table 1 and in Figure 1. In both trees, outgroups are not
 933 shown.

934

935 **FIGURE 4.**

936 The ancestral distribution areas obtained with the Bayesian binary Markov chain Monte
 937 Carlo (BBM) in RASP (Reconstruct Ancestral State in Phylogenies). Terminal nodes
 938 were assigned to seven geographical areas presented in the inset with different colours
 939 (see also map in Figure 1). Probabilities for reconstructions are given as percentages
 940 next to the proposed ancestral areas and are symbolised as pies. Terminal branches refer
 941 to the names of the geographic location/area of occurrence for the respective lineages.

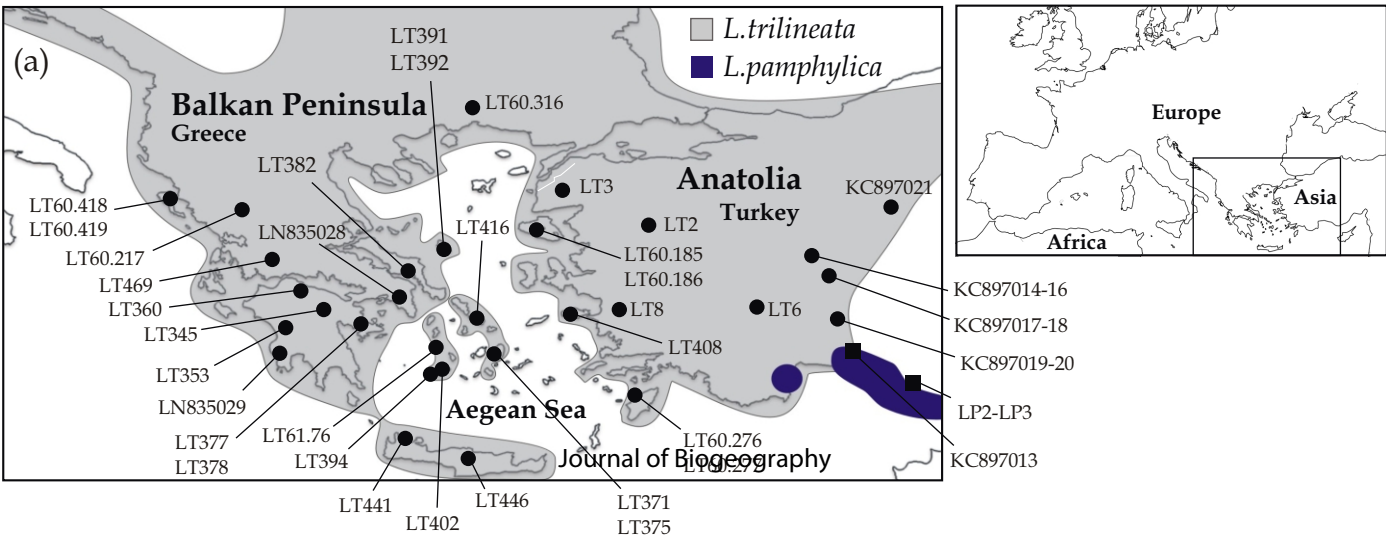
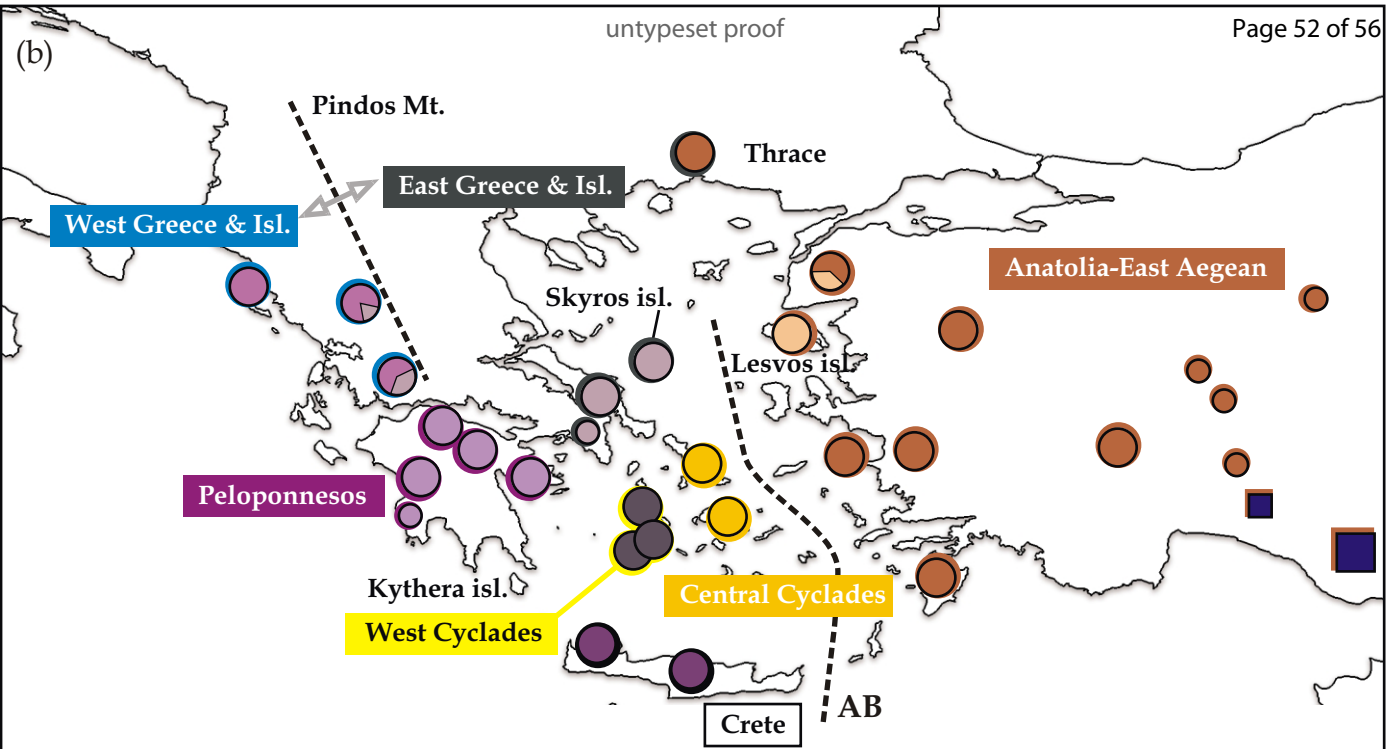
942

943 **FIGURE 5.**

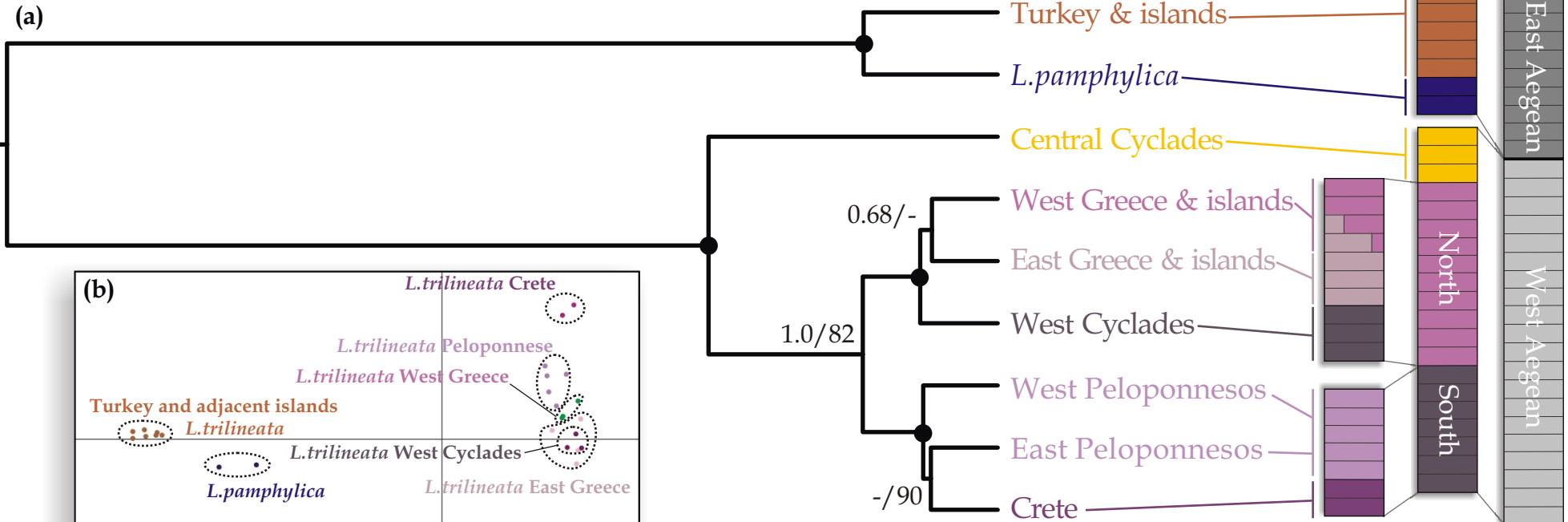
944 Dated mitochondrial gene-tree, based on complete cytochrome *b* sequences, inferred
 945 with BEAST (Bayesian Evolutionary Analysis Sampling Trees). Numbers next to nodes
 946 are mean ages and 95% intervals, both in Ma. Axis on the bottom refers to My. Nodes
 947 that represent the ancestors of species other than the target-species of the present study,

948 have been collapsed. Within the studied-group, each clade is a representative of each
949 mitochondrial cluster derived from the mPTP analysis (Multi-rate Poisson tree
950 processes). Names next to terminal branches refer to the geographic location/area the
951 respective lineages occur.

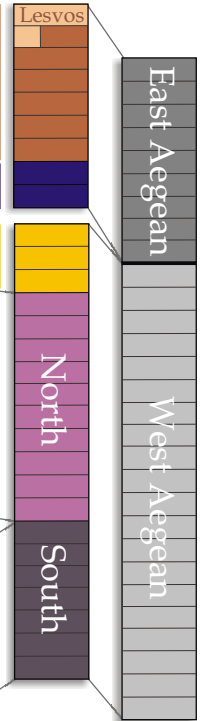
952



(a)



(c)



(b)

